



CHORUS

This is the accepted manuscript made available via CHORUS. The article has been published as:

Hidden Fermi Liquid, Scattering Rate Saturation, and Nernst Effect: A Dynamical Mean-Field Theory Perspective

Wenhu Xu, Kristjan Haule, and Gabriel Kotliar

Phys. Rev. Lett. **111**, 036401 — Published 17 July 2013

DOI: [10.1103/PhysRevLett.111.036401](https://doi.org/10.1103/PhysRevLett.111.036401)

Hidden Fermi Liquid, Scattering Rate Saturation, and Nernst Effect: a DMFT Perspective

Wenhu Xu,¹ Kristjan Haule,¹ and Gabriel Kotliar¹

¹*Department of Physics and Astronomy, Rutgers University, 136 Frelinghuysen Rd., NJ 08854*

We investigate the transport properties of a correlated metal within dynamical mean field theory. Canonical Fermi liquid behavior emerges only below a very low temperature scale T_{FL} . Surprisingly the quasiparticle scattering rate follows a quadratic temperature dependence up to much higher temperatures and crosses over to saturated behavior around a temperature scale T_{sat} . We identify these quasiparticles as constituents of the hidden Fermi liquid. The non-Fermi liquid transport above T_{FL} , in particular the linear-in- T resistivity, is shown to be a result of a strongly temperature dependent band dispersion. We derive simple expressions for resistivity, Hall angle, thermoelectric power and Nernst coefficient in terms of a temperature dependent renormalized band structure and the quasiparticle scattering rate. We discuss possible tests of the DMFT picture of transport using ac measurements.

PACS numbers: 71.10.Ay, 71.27.+a, 72.10.Bg

Fermi liquids [1] are good conductors. Quasiparticles (QP) with a mean free path much longer than their wavelength are responsible for the electric transport, and the resistivity vanishes quadratically at low temperatures. Landau theory is very robust and when reformulated in terms of a transport kinetic equation, it can be used to describe situations where Landau QPs are strictly speaking not well defined, namely when the QP scattering rate is comparable to their energy, such as the electron-phonon coupled system above the Debye temperature [2].

The metallic state of many strongly correlated materials is not described by Landau theory in a wide range of temperatures. Quadratic temperature dependence of resistivity occurs in a very narrow or vanishing range of temperatures. The interpretation of the resistivity in terms of the standard model of transport which is based on QPs is problematic since it leads to mean free paths shorter than the (QP) DeBroglie wavelength as stressed by Emery and Kivelson [3]. The transport properties of these “bad metals” thus requires a novel framework for their theoretical interpretation.

Dynamical mean field theory (DMFT) [4], provides a non-perturbative framework for the description of strongly correlated materials. It links observable quantities to a simpler, but still interacting, reference system (a quantum impurity in a self-consistent medium) rather than to a free electron system, hence it gives access to physical regimes outside the scope of Landau theory.

In a broad temperature range, the single-site DMFT description of the one band Hubbard model at large U and finite doping, results in transport and optical properties with anomalous temperature dependence [5–12], reminiscent of those observed in bad metals. Corresponding studies of half filled metallic systems [13–16] also reveal bad metallic behavior in a narrower temperature region since at high temperatures the resistivity is insulating like.

Landau QPs only emerge below an extremely low temperature, T_{FL} , which is much lower than the renormalized kinetic energy or Brinkman-Rice scale $T_{BR} \sim \delta W$

with δ the doping level and W the bare bandwidth. T_{BR} is the natural scale for the variation of physical quantities with doping at zero temperature [7, 17]. A recent comprehensive DMFT study of the Hubbard model with a semicircular bare density of states found that the transport properties above T_{FL} are described in terms of resilient QPs with a strong particle-hole asymmetry [11]. This asymmetry arises from the asymmetric pole structure in the self energy characterizing the proximity to the Mott insulator [18].

In this Letter we investigate the problem of bad metal transport. By expressing the DMFT transport coefficients in terms of QP quantities we find several surprising results: a) the QP scattering rate has a quadratic behavior for temperature much larger than T_{FL} and crosses over to a saturated behavior around T_{sat} . b) The temperature dependence of the transport coefficients is anomalous (in the sense that it does not reflect the T dependence of the QP scattering rate) and arises from the temperature dependent changes of the QP dispersion near the Fermi level. c) The temperature dependence of the QP dispersion affects differently the diagonal and off-diagonal charge and thermal transport coefficients but the Mott relation [19, 20] is valid when $T_{FL} < T < T_{sat}/2$.

We study the one-band Hubbard Hamiltonian on the two-dimensional square lattice with nearest neighbor hopping.

$$H = -t \sum_{\langle ij \rangle, \sigma} c_{i\sigma}^\dagger c_{j\sigma} + U \sum_i c_{i\uparrow}^\dagger c_{i\uparrow} c_{i\downarrow}^\dagger c_{i\downarrow}. \quad (1)$$

We set the full bare bandwidth $W = 8t$ to $W = 1$ as the unit of energy and temperature, and present results for $U/W = 1.75$, for which the system is a Mott insulator at half-filling. The doping level of the metallic state is fixed at $\delta = 15\%$ ($n = 0.85$). We use continuous time quantum Monte Carlo method (CTQMC) [21] and the implementation of ref. [22] to solve the auxiliary impurity problem. We use Padé approximants to analytically continue the self energy.

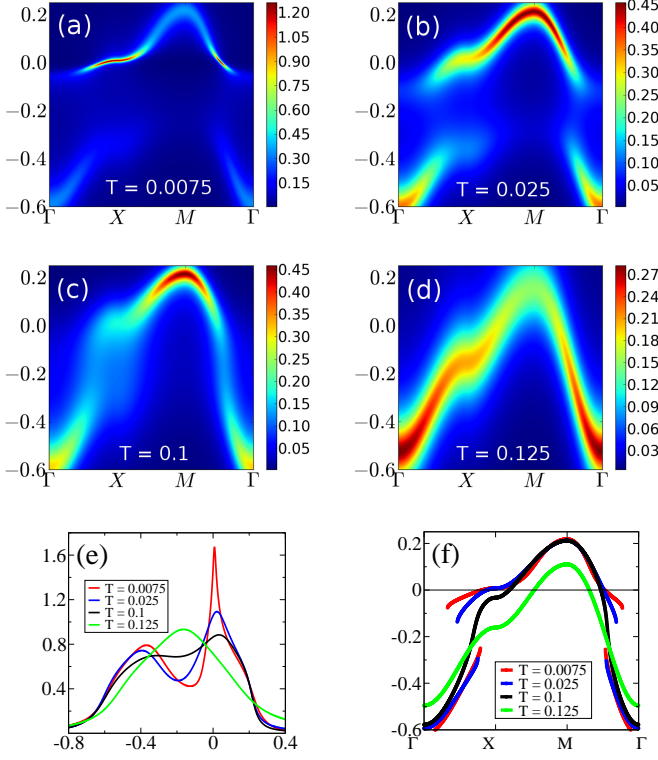


FIG. 1: Spectral function $A_{\mathbf{k}}(\omega)$ along $\Gamma - X - M - \Gamma$ in Brillouin zone at (a) $T = 0.0075$, (b) $T = 0.025$, (c) $T = 0.1$ and (d) $T = 0.125$. (e) Local density of states. (f) Roots of Eq. 3 at different temperatures.

The one-electron spectral function is defined as

$$A_{\mathbf{k}}(\omega) = -\frac{1}{\pi} \frac{\Im \Sigma(\omega)}{(\omega + \mu - \epsilon_{\mathbf{k}} - \Re \Sigma(\omega))^2 + \Im \Sigma(\omega)^2}, \quad (2)$$

in terms of the bare band dispersion $\epsilon_{\mathbf{k}} = -\frac{1}{4}(\cos(k_x) + \cos(k_y))$ and the self energy $\Sigma(\omega)$. $A_{\mathbf{k}}(\omega)$ at different temperatures are plotted in Fig. 1 (a-d).

Several characteristics of the evolution of $A_{\mathbf{k}}(\omega)$ with temperature are important. The solutions of the following equation,

$$\omega + \mu(T) - \epsilon_{\mathbf{k}} - \Re \Sigma(\omega, T) = 0, \quad (3)$$

faithfully reproduce the location of the peaks in $A_{\mathbf{k}}(\omega)$ and how they evolve with temperature (Fig. 1(f)). We do not describe in the following the upper Hubbard band at positive energies of order U .

There are two distinct temperature regimes separated by a crossover scale $T_{sat} \simeq 2T_{BR}/3 = 0.1$, which also sets the saturation scale of QP scattering rate as will be explained later. Above T_{sat} , say at $T = 0.125$, $A_{\mathbf{k}}(\omega)$ has one peak, i.e., Eq. 3 has only one root for each \mathbf{k} and displays a continuous dispersion over the whole Brillouin zone. Below T_{sat} , Eq. 3 can have multiple roots. The high temperature band breaks into two parts, which together with the upper Hubbard band form the characteristic DMFT three-peak structure of local density of

states (LDOS, Fig. 1(e)). The breakup of these bands also leads to the separation of the optical spectrum into a Drude peak and a mid-infrared feature, characteristic of many correlated systems, which provided the earliest experimental tests of the DMFT picture of correlated materials [5, 6, 13, 14].

There is always a dispersive QP feature in a $\sim k_B T$ energy window of the Fermi energy. $\omega_{\mathbf{k}}^*$ denotes the root of Eq. 3 closest to the Fermi level for a given \mathbf{k} . It evolves *continuously* with temperature from zero up to very high temperatures where there is no sharp peak in the LDOS (Fig. 1(e)). The dispersive excitations evolve continuously from strongly renormalized QPs located near the Luttinger Fermi surface with Fermi crossings around the X point and on the $\Gamma - M$ line for $T \ll T_{sat}$ (Fig. 1(a-b)), to holes in the lower Hubbard band (located near the M point) (Fig. 1(d)) for $T \gg T_{sat}$, as the spin degrees of freedom gradually unbind from the charge, with increasing temperature. The QP velocity is nearly temperature independent only below T_{FL} and above T_{sat} . The mass enhancement ($1/Z$), decreases with increasing temperature, from a large value ~ 5 below T_{FL} (Fig. 1(a)) to a value $\sim 1.5 \simeq (1 - n/2)^{-1}$ at high temperatures (Fig. 1(d)).

We now turn to the transport properties and focus on the electric current induced by electric fields and thermal gradients.

$$\mathbf{J}_e = \bar{\sigma}^0 \cdot \mathbf{E} - \bar{\sigma}^1 \cdot \nabla T. \quad (4)$$

$\bar{\sigma}^{0/1}$ is charge/thermal conductivity matrix. Several quantities of interest are resistivity(ρ), Hall angle(θ_H), Seebeck coefficient(S), and Nernst coefficient(ν) [20]. They are representative measures of longitudinal/transverse and magneto/thermo-electric transport properties and can be expressed in terms of elements of conductivity matrices,

$$\begin{aligned} \rho &= \frac{1}{\sigma_{xx}^0}, & \tan \theta_H &= -\frac{\sigma_{yx}^0}{\sigma_{xx}^0}, \\ S &= -\frac{\sigma_{yx}^1}{\sigma_{xx}^0}, & \nu &= -\frac{1}{B} \left(\frac{\sigma_{yx}^1}{\sigma_{xx}^0} - \frac{\sigma_{xx}^1 \sigma_{yx}^0}{(\sigma_{xx}^0)^2} \right). \end{aligned} \quad (5)$$

Within the DMFT treatment of the one-band Hubbard model, current vertex corrections vanish and the transport properties can be interpreted directly in terms of one-electron spectral function [5, 8, 9],

$$\begin{aligned} \sigma_{xx}^\alpha &= 2\pi \sum_{\mathbf{k}} \Phi_{\mathbf{k}}^{xx} \int d\omega \left(-\frac{\partial f(\omega)}{\partial \omega} \right) \left(\frac{\omega}{T} \right)^\alpha A_{\mathbf{k}}^2(\omega), \\ \frac{\sigma_{yx}^\alpha}{B} &= \frac{4\pi^2}{3} \sum_{\mathbf{k}} \Phi_{\mathbf{k}}^{yx} \int d\omega \left(-\frac{\partial f(\omega)}{\partial \omega} \right) \left(\frac{\omega}{T} \right)^\alpha A_{\mathbf{k}}^3(\omega), \end{aligned} \quad (6)$$

with $\alpha = 0$ or 1 for charge or thermal conductivity. We consider the limit of weak magnetic field, hence the off-diagonal conductivities are proportional to B . $\Phi_{\mathbf{k}}^{xx} = \epsilon_{\mathbf{k}}^{x2}$

and $\Phi_{\mathbf{k}}^{yx} = (\epsilon_{\mathbf{k}}^y)^2 \epsilon_{\mathbf{k}}^{xx} - \epsilon_{\mathbf{k}}^y \epsilon_{\mathbf{k}}^x \epsilon_{\mathbf{k}}^{yx}$ are transport functions in terms of bare band dispersion $\epsilon_{\mathbf{k}}$ and its derivatives. The derivatives are denoted by corresponding superscripts, $\epsilon_{\mathbf{k}}^\alpha = \partial \epsilon_{\mathbf{k}} / \partial k_\alpha$.

To recast Eqs. 6 in terms of QP, we linearize Eq. 3 at $\omega = \omega_{\mathbf{k}}^*$ and define $Z_{\mathbf{k}} = (1 - \frac{\partial \Re \Sigma(\omega)}{\partial \omega})^{-1} |_{\omega=\omega_{\mathbf{k}}^*}$. Then the low energy part of the one-electron Green's function can be approximated as

$$G_{\mathbf{k}}(\omega) \simeq \frac{Z_{\mathbf{k}}}{(\omega - \omega_{\mathbf{k}}^*) + i\Gamma_{\mathbf{k}}^*}. \quad (7)$$

Thus $Z_{\mathbf{k}}$ is the QP renormalization factor (or QP weight) and $\Gamma_{\mathbf{k}}^* = -Z_{\mathbf{k}} \Im \Sigma(\omega_{\mathbf{k}}^*)$ is the QP scattering rate.

Then the integrals in Eqs. 6 can be performed analytically and lead to

$$\begin{aligned} \sigma_{xx}^\alpha &\simeq \sum_{\mathbf{k}} \left(-\frac{\partial f(\omega)}{\partial \omega} \right)_{\omega_{\mathbf{k}}^*} \Phi_{\mathbf{k}}^{*xx} \left(\frac{\omega_{\mathbf{k}}^*}{T} \right)^\alpha \tau_{\mathbf{k}}^*, \\ \frac{\sigma_{yx}^\alpha}{B} &\simeq \frac{1}{2} \sum_{\mathbf{k}} \left(-\frac{\partial f(\omega)}{\partial \omega} \right)_{\omega_{\mathbf{k}}^*} \Phi_{\mathbf{k}}^{*yx} \left(\frac{\omega_{\mathbf{k}}^*}{T} \right)^\alpha (\tau_{\mathbf{k}}^*)^2. \end{aligned} \quad (8)$$

$\tau_{\mathbf{k}}^* = (\Gamma_{\mathbf{k}}^*)^{-1}$ is the QP lifetime. Transport functions are renormalized by $Z_{\mathbf{k}}$. $\Phi_{\mathbf{k}}^{*xx} = (\epsilon_{\mathbf{k}}^{*x})^2$ and $\Phi_{\mathbf{k}}^{*yx} = (\epsilon_{\mathbf{k}}^{*y})^2 \epsilon_{\mathbf{k}}^{*xx} - \epsilon_{\mathbf{k}}^{*y} \epsilon_{\mathbf{k}}^{*x} \epsilon_{\mathbf{k}}^{*yx}$, with $\epsilon_{\mathbf{k}}^{*\alpha(\beta)} = Z_{\mathbf{k}} \epsilon_{\mathbf{k}}^{\alpha(\beta)}$ ($\alpha, \beta = x, y$).

This reformulation leads to a transparent interpretation in terms of QPs with temperature dependent dispersion $\omega_{\mathbf{k}}^*$. Eqs. 8 has a form similar to the solution of the kinetic equations from Boltzmann theory [23]. The essential difference from the Prange-Kadanoff treatment of the electron-phonon problem [2] is the strong temperature dependence of the QP dispersion brought in by $Z_{\mathbf{k}}$.

First we validate the simplified description of transport, Eqs. 8 (“QP approx.”), by benchmarking it against the results of the exact DMFT expressions, Eqs. 6 (“exact exp.”), for the resistivity, Hall angle, Seebeck, and Nernst coefficients. The quantitative agreement between Eqs. 8 and Eqs. 6 is evident, as shown in Fig. 2(a-d). The QP approximation faithfully reproduces the results of all transport quantities over the whole temperature range, extending to temperatures well above T_{sat} .

Fig. 3(a) shows the QP scattering rate on Fermi surface, i.e., $\Gamma_{\mathbf{k}_F}^*$ with $\omega_{\mathbf{k}_F}^* = 0$ (For later use we also write $\tau_{\mathbf{k}_F}^* = (\Gamma_{\mathbf{k}_F}^*)^{-1}$ as the QP lifetime and $Z_{\mathbf{k}_F}$ as the renormalization factor at Fermi surface). T_{sat} demarcates the non-monotonic temperature dependence of $\Gamma_{\mathbf{k}_F}^*$. Below T_{sat} , $\Gamma_{\mathbf{k}_F}^*$ increases and reaches maximum at T_{sat} . Above T_{sat} , $\Gamma_{\mathbf{k}_F}^*$ decreases very slowly and eventually approaches to a value moderately smaller than the maximum. This confirms that T_{sat} characterizes the crossover between two distinct scattering behaviors. The inset of Fig. 3(a) shows estimated values of $(k_F l^*)^{-1}$ with k_F an estimation of the average Fermi momentum by assuming a circular Fermi surface containing $(1 - \delta)/2$ electrons per spin and with $l^* = v_{\mathbf{k}_F}^* \tau_{\mathbf{k}_F}^*$ the QP mean free path, where $v_{\mathbf{k}_F}^* = \sqrt{\langle v_{\mathbf{k}}^2 \rangle}$ with $\langle \dots \rangle$ averaging over the

Fermi level. At low temperatures, $(k_F l^*)^{-1}$ increases with temperature, as expected in a good metal, and crosses over to a much slower increase, or saturated behavior around $T_{sat}/2$. Above $T_{sat}/2$, $(k_F l^*)^{-1} \simeq 0.5$, and does not exceed the Mott-Ioffe-Regel (MIR) bound, which states that $(k_F l^*)^{-1} < 1$ in a metal. The QPs behave as expected in Boltzmann transport theory in the full temperature range, reaching the non-degenerate limit at $T \gg T_{sat}$. Notice that above T_{FL} , $\Im \Sigma(0)$ is not quadratic in temperature, only $\Gamma_{\mathbf{k}_F}^* = -Z_{\mathbf{k}_F} \Im \Sigma(0)$ is quadratic.

The anomalies in the transport properties are the result of the strong temperature dependence of the renormalized dispersion. This is best understood by means of a general Sommerfeld expansion of Eqs. 8, which is explained in Supplementary Material and works well below $T_{sat}/2$. For this purpose we define $\Phi^{*xx/yx}(\epsilon) = \sum_{\mathbf{k}} \Phi_{\mathbf{k}}^{*xx/yx} \delta(\epsilon - \omega_{\mathbf{k}}^*)$ and the energy dependent QP lifetime $\tau^*(\epsilon) = \tau_{\mathbf{k}}^*$ when $\epsilon = \omega_{\mathbf{k}}^*$, with scattering rate $\Gamma^*(\epsilon) = (\tau^*(\epsilon))^{-1}$. For $|\epsilon| \lesssim T$, $\Phi^{*xx/yx}(\epsilon)$ is expanded to the linear order in ϵ . To keep the asymmetry in $\Gamma^*(\epsilon)$, which is important for the thermoelectric transport, we expand $\Gamma^*(\epsilon)$ to cubic order of ϵ , and treat the linear and cubic order as corrections to the zeroth and quadratic terms, which are dominant in the Fermi liquid regime at low temperatures. The insets in Fig. 2 compare the estimation using this expansion (purple dots) and the results of the full expressions (black dots). The agreement is evident and the expansion quantitatively captures the variation below $T_{sat}/2$.

The inset of Fig. 2(a) shows the linearity of resistivity, a typical non-Fermi liquid behavior [24], up to $T_{sat}/4 \simeq 0.025$, as indicated by the linear fitting (blue dashed line). Surprisingly the QP scattering rate $\Gamma_{\mathbf{k}_F}^*$ has a quadratic temperature dependence also up to $T_{sat}/4$ (Fig. 3(b)). This is due to the strong temperature dependence of $Z_{\mathbf{k}_F}$ (Fig. 3(c)). In fact, the leading order in the general Sommerfeld expansion gives

$$\rho \simeq (Z_{\mathbf{k}_F} \Phi^{xx}(\tilde{\mu}) \tau_{\mathbf{k}_F}^*)^{-1}, \quad (9)$$

where $\Phi^{xx}(\tilde{\mu}) = \sum_{\mathbf{k}} \Phi_{\mathbf{k}}^{xx} \delta(\tilde{\mu} - \epsilon_{\mathbf{k}})$ with $\tilde{\mu} = \mu - \Re \Sigma(0)$ and we have used $\Phi^{*xx}(0) = Z_{\mathbf{k}_F} \Phi^{xx}(\tilde{\mu})$. $Z_{\mathbf{k}_F} \simeq 0.1 + 12T$ for $T_{FL} < T < T_{sat}/4$, leads to the quasilinear resistivity and also affects all other transport coefficients in Eqs. 8. The temperature dependence of $Z_{\mathbf{k}_F}$ becomes negligible only below the Fermi liquid temperature $T_{FL} \simeq T_{sat}/15$. $\Phi^{xx}(\tilde{\mu})$ is very weakly temperature dependent as shown in the inset of Fig. 3(c). Above T_{sat} , the resistivity is quasilinear in temperature with a slope smaller than that below $T_{sat}/4$, while the QP scattering rate is saturated. The general Sommerfeld expansion cannot be used at high temperatures, but the discrepancy between the scattering rate and resistivity can be traced to the variation of $\tilde{\mu}$ with temperature, leading to the shift of QP band relative to the Fermi window $-\partial f(\omega)/\partial \omega$.

Similarly, the leading order in the Hall angle (Fig. 2(b)) is given by $\tan \theta_H / B \simeq Z_{\mathbf{k}_F} \Phi^{yx}(\tilde{\mu}) \tau_{\mathbf{k}_F}^* / 2\Phi^{xx}(\tilde{\mu})$ and indicates the sign change at $T \simeq T_{sat}/4$ is due to the sign

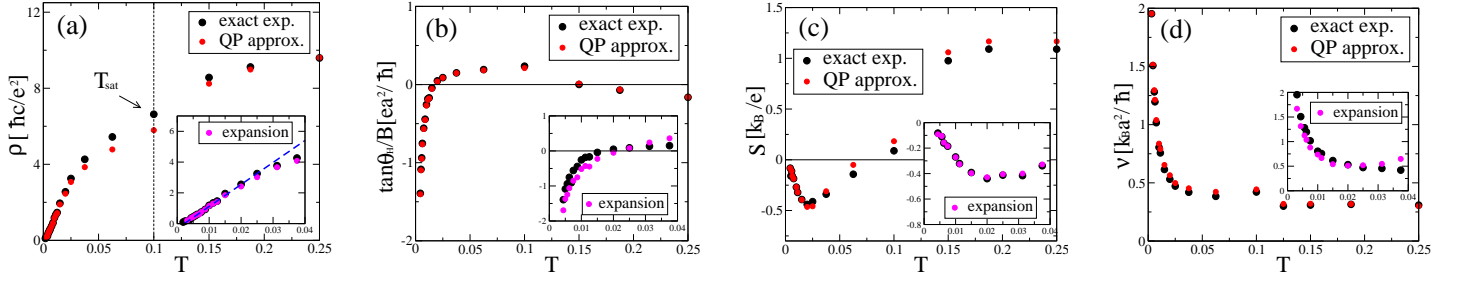


FIG. 2: Transport properties. (a) Resistivity. (b) Hall angle. (c) Seebeck coefficient. (d) Nernst coefficient. “exact exp.” are obtained using Eqs. 6. “QP approx.” are obtained using Eqs. 8. “expansion” are obtained using the general Sommerfeld expansion detailed in Supplementary Material. The units are expressed in terms of universal constants, \hbar , k_B , e , and in-plane/out-of-plane lattice constant, a/c .

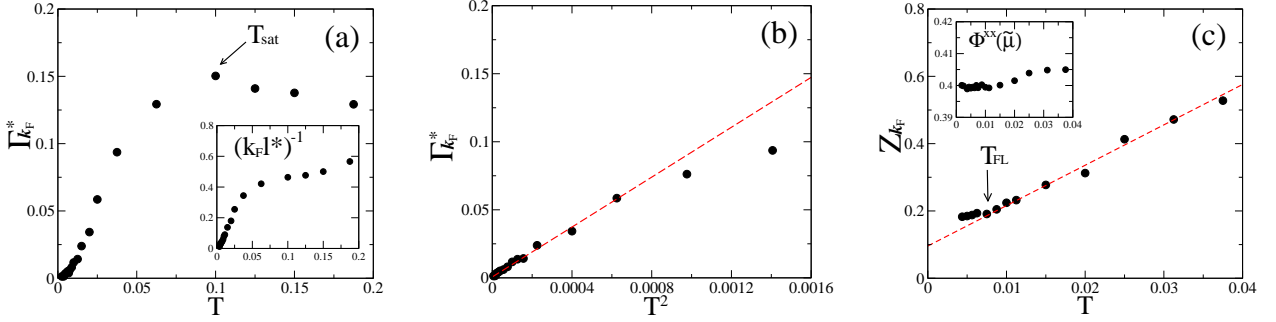


FIG. 3: (a) Quasiparticle scattering rate $\Gamma_{\mathbf{k}_F}^*$. The inset shows the estimation of $(k_F l^*)^{-1}$. (b) $\Gamma_{\mathbf{k}_F}^*$ as a function of T^2 for $T \lesssim T_{sat}/2$. (c) Quasiparticle renormalization factor $Z_{\mathbf{k}_F}$ for $T \lesssim T_{sat}/2$.

change in $\Phi^{yx}(\tilde{\mu})$, a consequence of the evolution of Fermi surface from a hole-like one to an electron-like one. For the Seebeck coefficient (Fig. 2(c)), the expansion leads to

$$S \simeq \left(-\frac{\pi^2}{3} T \right) \left(\frac{d \ln \Phi^{*xx}(0)}{d\epsilon} + \frac{d \ln \tau^*(0)}{d\epsilon} \right). \quad (10)$$

The asymmetry in scattering rate competes with the asymmetry in the QP band structure, hence instead of sign change, S shows non-monotonic temperature dependence below $T_{sat}/2$.

The Nernst coefficient ν (Fig. 2(d)) rises steeply below $T_{sat}/4$, and provides a good probe of the temperature dependence of $\tau_{\mathbf{k}_F}^*$. The leading orders in the expansion gives

$$\nu \simeq \left(-\frac{\pi^2}{3} T \right) \left[\tau_{\mathbf{k}_F}^* \frac{d}{d\epsilon} \left(\frac{\Phi^{*yx}(0)}{\Phi^{*xx}(0)} \right) + \frac{\Phi^{*yx}(0)}{\Phi^{*xx}(0)} \frac{d\tau^*(0)}{d\epsilon} \right]. \quad (11)$$

In the square lattice near half-filling, the asymmetry in band structure dominates and leads to $\nu \propto \tau_{\mathbf{k}_F}^* T \propto 1/T$. This rise is seen in many materials [20] before ν drops linearly in T at very low temperature [37].

Further studies should be carried out to ascertain to which extent the DMFT description of transport applies to real materials, but the strong similarities between the experimental features revealed in the phenomenological picture in ref. [24] and our results are encouraging. AC transport measurements can be used

to extract the temperature dependence of $\tau_{\mathbf{k}_F}^*$. At low frequency, the optical conductivity is parametrized as [25, 26] $\sigma(\omega) = \frac{\omega_{opt}^{*2}}{4\pi} \left(-i\omega + \frac{1}{\tau_{opt}^*} \right)^{-1}$, with $\omega_{opt}^{*2} \simeq 8\pi\Phi^{*xx}(0) = 8\pi Z_{\mathbf{k}_F} \Phi^{xx}(\tilde{\mu})$ and $\tau_{opt}^* \simeq \tau_{\mathbf{k}_F}^*/2$. Similarly in AC Hall effect [27], $\tan \theta_H(\omega)/B = \frac{\omega_H^{*2}}{4\pi} \left(-i\omega + \frac{1}{\tau_H^*} \right)^{-1}$ follows, with $\omega_H^{*2} \simeq 4\pi \frac{\Phi^{*yx}(0)}{\Phi^{*xx}(0)} = 4\pi \frac{Z_{\mathbf{k}_F} \Phi^{yx}(\tilde{\mu})}{\Phi^{xx}(\tilde{\mu})}$ and $\tau_H^* \simeq \tau_{\mathbf{k}_F}^*/2$. Frequency dependent thermoelectric measurements would give additional information on the asymmetry of the QP dispersion and scattering rate.

The extension from model Hamiltonians to the LDA+DMFT framework is straightforward. It can be used to separate the temperature dependence of transport coefficients arising from the temperature dependence of the QP band and that of the scattering rate, in materials such as the ruthenates [28], the vanadates [29] and the nickelates [14, 30, 31] for which the LDA+DMFT description is known to provide an accurate zeroth order picture of numerous properties [14]. Recent experiments on cuprates [32] have revealed evidence for temperature dependence of ω_{opt}^{*2} and a T^2 -scattering rate over a broad range of temperatures. These materials require cluster DMFT studies to describe their momentum space differentiation. Still, it is tempting to interpret the transport properties in terms of QPs to provide an effective description of the transport. Indeed the QP scattering rate computed in the t-J model in ref. [33], exhibits the sat-

uration behavior described in this work and it would be interesting to re-analyze the results in terms of the QPs of the hidden Fermi liquid. Our findings are related to two earlier theoretical proposals. Anderson introduced the idea of a hidden Fermi liquid [34, 35], requiring $Z_{\mathbf{k}_F}$ strictly vanishing at $T = 0$ in the normal state. Alternatively, our results could be cast into the framework of the

extremely correlated Fermi liquid [36] by the temperature dependence of the caparison function.

Acknowledgement: this work was supported by NSF grant No. DMR-0906943 and No. DMR-0746395. We acknowledge useful discussions with D. N. Basov, X. Y. Deng, A. Georges, A. Kutepov, J. Mravlje, and A.-M. S. Tremblay.

-
- [1] L. Landau, Sov. Phys. JETP **3**, 920 (1957).
 [2] R. E. Prange and L. P. Kadanoff, Phys. Rev. **134**, A566 (1964).
 [3] V. J. Emery and S. A. Kivelson, Phys. Rev. Lett. **74**, 3253 (1995).
 [4] A. Georges, G. Kotliar, W. Krauth, and M. J. Rozenberg, Rev. Mod. Phys. **68**, 13 (1996).
 [5] T. Pruschke, D. L. Cox, and M. Jarrell, Phys. Rev. B **47**, 3553 (1993).
 [6] T. Pruschke, M. Jarrell, and J. Freericks, Advances in Physics **44**, 187 (1995).
 [7] H. Kajueter, G. Kotliar, and G. Moeller, Phys. Rev. B **53**, 16214 (1996).
 [8] G. Pálsson and G. Kotliar, Phys. Rev. Lett. **80**, 4775 (1998).
 [9] E. Lange and G. Kotliar, Phys. Rev. B **59**, 1800 (1999).
 [10] W. Xu, C. Weber, and G. Kotliar, Phys. Rev. B **84**, 035114 (2011).
 [11] X. Deng, J. Mravlje, R. Zitko, M. Ferrero, G. Kotliar, and A. Georges, Phys. Rev. Lett. **110**, 086401 (2013).
 [12] L.-F. Arsenault, B. S. Shastry, P. Sémon, and A.-M. S. Tremblay, Phys. Rev. B **87**, 035126 (2013).
 [13] M. J. Rozenberg, G. Kotliar, H. Kajueter, G. A. Thomas, D. H. Rapkine, J. M. Honig, and P. Metcalf, Phys. Rev. Lett. **75**, 105 (1995).
 [14] J. Merino and R. H. McKenzie, Phys. Rev. B **61**, 7996 (2000).
 [15] P. Limelette, P. Wzietek, S. Florens, A. Georges, T. A. Costi, C. Pasquier, D. Jérôme, C. Mézière, and P. Batail, Phys. Rev. Lett. **91**, 016401 (2003).
 [16] J. Merino, M. Dumm, N. Drichko, M. Dressel, and R. H. McKenzie, Phys. Rev. Lett. **100**, 086404 (2008).
 [17] D. S. Fisher, G. Kotliar, and G. Moeller, Phys. Rev. B **52**, 17112 (1995).
 [18] P. Grete, S. Schmitt, C. Raas, F. B. Anders, and G. S. Uhrig, Phys. Rev. B **84**, 205104 (2011).
 [19] M. Jonson and G. D. Mahan, Phys. Rev. B **21**, 4223 (1980).
 [20] K. Behnia, Journal of Physics: Condensed Matter **21**, 113101 (2009).
 [21] P. Werner, A. Comanac, L. de' Medici, M. Troyer, and A. J. Millis, Phys. Rev. Lett. **97**, 076405 (2006).
 [22] K. Haule, Phys. Rev. B **75**, 155113 (2007).
 [23] N. W. Ashcroft and N. D. Mermin, *Solid State Physics* (Saunders College, Philadelphia, 1976).
 [24] N. Hussey, K. Takenaka, and H. Takagi, Philosophical Magazine **84**, 2847 (2004).
 [25] D. Van der Marel, H. Molegraaf, J. Zaanen, Z. Nussinov, F. Carbone, A. Damascelli, H. Eisaki, M. Greven, P. Kes, M. Li, et al., Nature **425**, 271 (2003).
 [26] D. N. Basov, R. D. Averitt, D. van der Marel, M. Dressel, and K. Haule, Rev. Mod. Phys. **83**, 471 (2011).
 [27] H. Drew, S. Wu, and H. S. Lihn, Journal of Physics: Condensed Matter **8**, 10037 (1996).
 [28] J. Mravlje, M. Aichhorn, T. Miyake, K. Haule, G. Kotliar, and A. Georges, Phys. Rev. Lett. **106**, 096401 (2011).
 [29] R. Arita, K. Held, A. V. Lukoyanov, and V. I. Anisimov, Phys. Rev. Lett. **98**, 166402 (2007).
 [30] M. K. Stewart, C.-H. Yee, J. Liu, M. Kareev, R. K. Smith, B. C. Chapler, M. Varela, P. J. Ryan, K. Haule, J. Chakhalian, et al., Phys. Rev. B **83**, 075125 (2011).
 [31] X. Deng, M. Ferrero, J. Mravlje, M. Aichhorn, and A. Georges, Phys. Rev. B **85**, 125137 (2012).
 [32] S. I. Mirzaei, D. Stricker, J. N. Hancock, C. Berthod, A. Georges, E. van Heumen, M. K. Chan, X. Zhao, Y. Li, M. Greven, et al., ArXiv e-prints (2012), 1207.6704.
 [33] K. Haule and G. Kotliar, Phys. Rev. B **76**, 104509 (2007).
 [34] P. W. Anderson, Phys. Rev. B **78**, 174505 (2008).
 [35] P. A. Casey and P. W. Anderson, Phys. Rev. Lett. **106**, 097002 (2011).
 [36] B. S. Shastry, Phys. Rev. Lett. **107**, 056403 (2011).
 [37] Disorder in real materials cuts off the divergence of $\tau_{\mathbf{k}_F}^*$ and ν is thus linear in T at very low temperatures. This linearity is sometimes taken as a signature of Fermi-liquid behavior.